PCCP

Accepted Manuscript

ROYAL SOCIETY OF CHEMISTRY

www.rsc.org/pccp

Ultrafast Charge Carrier Relaxation and Charge Transfer Processes in CdS/CdTe Thin Films

Bill Pandit,[†,‡,§] Ruvini Dharmadasa,[‡] I. M. Dharmadasa,[¶] Thad Druffel,[‡] and Jinjun Liu[*,†,‡]

Department of Chemistry, University of Louisville, Louisville, Kentucky 40292, USA, Conn Center for Renewable Energy Research, University of Louisville, Louisville, Kentucky, 40292, USA, and Electronic Materials and Sensors Group, Materials and Engineering Research Institute, Sheffield Hallam University, Sheffield S1 1WB, UK

E-mail: j.liu@louisville.edu

May 10, 2015

[*]To whom correspondence should be addressed
[†]Department of Chemistry, University of Louisville, Louisville, Kentucky 40292, USA
[‡]Conn Center for Renewable Energy Research, University of Louisville, Louisville, Kentucky, 40292, USA
[¶]Electronic Materials and Sensors Group, Materials and Engineering Research Institute, Sheffield Hallam University, Sheffield S1 1WB, UK
[§]Current address: Department of Chemistry, Northwestern University

Abstract

Ultrafast transient absorption pump-probe spectroscopy (TAPPS) has been employed to investigate charge carrier relaxation in cadmium sulfide/cadmium telluride (CdS/CdTe) nanoparticle (NP)-based thin films and electron transfer (ET) processes between CdTe and CdS. Effects of post-growth annealing treatments to ET processes have been investigated by carrying out TAPPS experiments on three CdS/CdTe samples: as deposited, heat treated, and $CdCl_2$ treated. Clear evidence of ET process in the treated thin films has been observed by comparing transient absorption (TA) spectra of CdS/CdTe thin films to those of CdS and CdTe. Quantitative comparison between ultrafast kinetics at different probe wavelengths unravels the ET processes and enables determination of its rate constants. Implication of the photoinduced dynamics to photovoltaic devices is discussed.

Keywords: ultrafast laser spectroscopy, transient absorption, interface defects, $CdCl_2$ post-growth annealing treatment, band-filling effect.

Figure of Content:

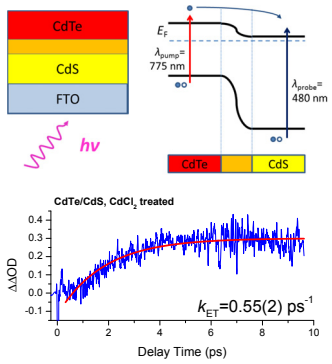

Charge transfer processes in CdS/CdTe thin films have been studied by femtosecond transient absorption spectroscopy.

1 Introduction

Cadmium telluride (CdTe) is one of the leading thin film materials for photovoltaic (PV) applications.[1,2] The advantage of using CdTe in thin-film solar cells lies on the fact that it is a direct band gap material with high absorption compared to silicon and the ease of device processing and high stability. It can be deposited on conducting glass in thin film form with a typical thickness of a few microns at low temperature. The CdS/CdTe heterojunction with CdTe as the absorber layer and CdS as the window layer remains as one of the most promising structures for the production of low-cost PV modules. Although the efficiency of CdS/CdTe thin-film solar cells was stagnated at ∼16%[3,4] for the last two decades, during the past 2-3 years, the efficiency has rapidly increased from ∼16% to 21.5%.[5] However, this efficiency is still lower than the theoretical maximum efficiency of 29% for a single-band-gap CdTe junction.[6,7] Unraveling the charge carrier relaxation and charge transfer (CT) processes in CdS/CdTe thin films is therefore of high significance for further progress. CdS/CdTe heterojunction is also used to make type II core-shell quantum dots (QDs)[8–10] as well as nanorods.[11] The CdS/CdTe QD is particularly attractive because of the high efficiency of charge transfer across its interface, which gives the potential benefits in optoelectronics devices and future QD-sensitized solar cells.

Charge carrier relaxation and CT processes in CdS/CdTe QDs have been investigated by ultrafast laser spectroscopy.[8–10] Both electron transfer from the conduction band of CdTe to CdS[8] and hole transfer from the valence band of CdS to CdTe[10] have been observed in ultrafast transient absorption spectroscopy measurements. It has been shown that the charge transfer processes are affected by thickness of the CdS shell. However, fewer transient absorption spectroscopy measurements have been carried out on CdS and CdS/CdTe thin films.[12] The objective of the present investigation is therefore to unravel the photoinduced processes in CdS/CdTe thin films using the transient absorption technique. Steady-state UV/visible absorption spectra and photoluminescence (PL) spectra were also obtained to help interpret the ultrafast spectroscopy results. Furthermore, CdS and CdTe thin films

were studied for comparison.

Performance of a heterojunction depends on thin film deposition and subsequent processing.[13–16] The resulting interface structure plays an important role in charge transfer. In the CdS/CdTe heterojunction, a $CdS_xTe_{1-x}/CdTe_yS_{1-y}$ interface layer is formed by interdiffusion and interaction. $CdCl_2$ treatment or "junction activation" increases the atomic mobility of CdS or CdTe at the annealing temperature *via* different mechanisms including grain growth, passivation of interface defects, and changing the abrupt junction into a graded one.[17] Heat treatment at low temperature improves crystallinity and purity.[18] Recently, intense pulsed light (IPL) treatment was applied on CdTe nanoparticle thin films.[15,19] Upon IPL treatment with an optimized pulse energy, optimum recrystallization and decrease in defects were achieved. Grains as large as 2 μm were observed. IPL-treated CdTe thin films are therefore of potential benefit in producing thin-film solar cells with high efficiency. In order to determine the effects of different sample treatment processes on charge carrier relaxation and especially CT processes, three types of CdS/CdTe films: as deposited, heat treated, and $CdCl_2$ treated, were studied in transient absorption experiment and their spectra are compared, which demonstrates different photoinduced processes.

2 Experimental

2.1 Preparation of as-deposited CdS, CdTe and CdS/CdTe thin films

Thin films of CdS and CdTe were deposited using 2-electrode cathodic electrochemical deposition onto fluorinated tin oxide glass substrates (FTO, Tec 8, Hartford Glass Inc.).[13,19] CdS was deposited from an aqueous 0.3 M cadmium chloride ($CdCl_2$, Sigma Aldrich) solution, using sodium thiosulfate as the sulfur source. The pH of the bath was lowered to pH=2.00 using hydrochloric acid. The films were grown at 1.500 V to produce slightly cadmium rich films. CdTe was also deposited from an aqueous bath, however in this case 0.5 M

cadmium sulfate ($CdSO_4$, Sigma Aldrich) and a dilute solution of tellurium dioxide (TeO_2, Sigma Aldrich) were used as the cadmium and tellurium sources, respectively. The CdTe films were grown at a pH of 1.44 and growth voltage of 1.701 V. The thickness of the films was controlled by varying the growth time and was measured using a Technor Instruments Alpha-Step 500 surface profiler. CdS/CdTe films were grown under the same conditions described above. However prior to CdTe deposition, the CdS films were heat treated with $CdCl_2$ (Section 2.2). It is worth noting that ∼100 nm thick CdTe layer used in the present work is not fully formed as the material used in complete devices, which normally has a thickness of ∼1.5 μm. The layers used here are in early stages of formation, and therefore consists of nano-particles.

2.2 Heat treatment with and without cadmium chloride

Heat Treatment without $CdCl_2$: The samples were heat treated on a hot plate in atmospheric conditions, first from room temperature to 100°C for 5 minutes and then to 400°C for 10 minutes. They were then allowed to cool on the hotplate for 10 minutes.

Heat Treatment with $CdCl_2$: Prior to heat treatment, a saturated aqueous solution of cadmium chloride ($CdCl_2$, Sigma Aldrich) was spread over the surface of the films and allowed to dry. The samples were then heated following the method described above.

2.3 Steady-state UV/visible absorption and photoluminescence spectroscopy

UV/visible absorption spectra of CdS/CdTe thin films were obtained using a Perkin Elmer Lambda 950 UV/Vis/NIR spectrometer. PL spectra were obtained using a Renishaw InVia Raman microscope with the 442 nm output from a Helium-Cadmium laser used as the excitation source.

2.4 Ultrafast transient absorption pump-probe spectroscopy (TAPPS)

Ultrafast TAPPS measurements were performed on CdS, CdTe and CdS/CdTe thin films. The TAPPS system[20] uses an ultrafast Ti:Sapphire laser amplifier system (Clark-MXR, ShapeShifter, wavelength=775 nm, pulse duration$\lesssim$150 fs, pulse energy$\sim$1 mJ at 1 kHz repetition rate). For the present experiment, pump sources with two different wavelengths were used: (i) output of the regenerative amplifier (775 nm) and (ii) second harmonics of the CPA output (388 nm) by frequency doubling in a BBO crystal. A neutral density filter attenuates the pump beams and a fluence of $\sim$20 μJ/cm^2 was used for all TA spectra reported in this paper. Part of the CPA output is also separated to pump a 3 mm-thick sapphire plate to generate supercontinuum white-light (420-1600 nm), which is used as the probe source. Transmission of the probe beam is dispersed by a curved grating and detected by a linear array CMOS detector in the wavelength range of 430 nm to 730 nm. The pump beam is modulated by an optical chopper revolving at 500 Hz, half of the repetition rate of the femtosecond laser, and the transient absorption (TA) signal is recorded as the change in optical density (ΔOD) with pump beam blocked and unblocked. Time delay between pump and probe pulses (Δt) is variable by moving a retroreflector on a computer-controlled translation stage which reflects the pump beam. All TAPPS measurements were performed by pumping the sample from the glass/FTO substrate side to reduce the heating effect. For CdS/CdTe thin films, the laser beams transmit through the CdS layer before they reach the CdTe layer.

3 Results

3.1 Steady-state UV/visible absorption

The band gaps of CdS and CdTe bulk semiconductor at room temperature are 2.42 eV (512 nm)[21] and 1.44 eV (861 nm),[22] respectively. CdS and CdTe nanoparticle (NP)-based thin

films made by electrochemical deposition show slightly higher values due to quantum effects (2.46 eV for CdS and 1.51 eV for CdTe). These increased band gap values can also be arise due to transmission of light through pin-holes in very thin layers used in this work. UV/visible absorption spectra of FTO, FTO/CdS, and FTO/CdTe are given in the Supplementary Information (Figure S.1 and S.2). For all three CdS/CdTe samples (as deposited, heat treated, and $CdCl_2$ treated), the absorption spectra (Figure 1) are dominated by strong absorption of CdS, presented as a step at ∼490 nm (2.53 eV). The baselines that extend into near-IR region is attributed mainly to CdTe absorption.

3.2 Photoluminescence spectroscopy

Figure 2 shows the PL spectra of glass/FTO/CdS/CdTe structure at room temperature, while those of FTO, FTO/CdS, and FTO/CdTe are given in the Supplementary Information (Figure S.3 and S.4). Measurements were confined to a photon energy range of 1.30 eV to 3.00 eV. The peak appearing at ∼2.42 eV corresponds to the band-to-band electron transitions of CdS. This value is close to the reported energy band gap of bulk CdS material. The highest intensity peak occurs at a value of ∼1.48 eV, which corresponds to the band-to-band transition in the CdTe material. This energy gap is close to the reported band gap of CdTe thin films. However, this peak covers the range from 1.30 eV to 1.70 eV, indicating contributions from donor-to-acceptor and donor-to-valence band transitions. This suggests that the material contains numerous shallow defects close to the conduction and valence bands, which causes the redshift of the band gap. The spread toward 1.70 eV could arise from the combination of quantum effects from nano-crystalline particles of CdTe. Another effect will appear from the presence of CdS_xTe_{1-x} alloy at the interface, which will have a higher energy gap than that of the net CdTe thin film (∼1.48 eV). The broad shoulder at ∼2.08 eV could arise from the phase of CdS_xTe_{1-x} alloy or defect level present in the CdS layer.

The band to band transition of CdTe (1.48 eV) in the PL spectrum of the CdS/CdTe

thin film after heat treatment in air without $CdCl_2$ resulted in a relative decrease in intensity compared to that treated with $CdCl_2$ (Figure 2). This result indicates that $CdCl_2$ is needed during heat treatment to avoid deterioration of the films properties. During heat treatment without $CdCl_2$, the CdTe layer deteriorates due to loss of material through sublimation. In the presence of $CdCl_2$, the CdTe layer improves in every aspect: Recrystallization, removal of defects, and drastic enhancement of device efficiencies are experimentally observed, although a full understanding of the mechanisms is not yet achieved. The heat treatment with $CdCl_2$ improves the electrical and optical properties of the CdTe layer too. The increase in the intensity of the band-to-band transition and reduction in the peak width are positive indications of the decrease in shallow defects in the band gap. This is one of the main reasons why the CdS/CdTe solar cell efficiencies increase after $CdCl_2$ treatment.

3.3 TA spectra of CdS and CdTe thin films

As a control, TA spectra of CdS and CdTe thin films were obtained with pump photon energies above their respective band gaps. The CdTe thin film was excited by a 775 nm (1.60 eV) pump beam. The TA spectra using a white-light probe beam show mostly only positive signals (Figure 3a) that is attributed to photoinduced absorption (PA) of CdTe. Figure 3b shows the transient kinetics at three different probe wavelengths of 450, 480 and 650 nm. The kinetics at all wavelengths are triphasic, exhibiting a fast decay with time constant ~5 ps that dominates the first 20 ps, a slow decay that extends to ~ 500 ps, and a decay with an intermediate rate afterwards. The fast decay is attributed to charge carrier trapping. The decay constants are significantly different for different wavelengths and are in general smaller at shorter wavelengths, indicating faster trapping. The two slower decay components are due to recombination of charge carriers. Toward the short wavelength limit of the array detector (~430 nm), a negative signal was observed ~5 ps after photoexcitation. (See, for instance, the kinetics at 480 nm and 450 nm in Figure 3b). Such a negative signal is assigned to ground-state photobleaching (PB) as the wavelengths are shorter than that of

the pump source. The negative signal toward the long-wavelength limit of the array detector (∼730 nm), is attributed to stimulated emission (SE) because it is consistent with the strong CdTe peak in the PL spectra in the same region (Figure 2).

TA spectra of CdS were also obtained using 388 nm (3.20 eV) pump beam (Figure 4a). A strong negative signal was observed around 480 nm, consistent with the ∼490 nm step in the steady-state absorption spectrum (Figure 1). Previously, excition dynamics of CdS thin films produced by chemical bath deposition (CBD) and DC pulse sputtering (DCPS) has been investigated by TAPPS with 460 nm pumping.[12] The observed negative TA signal was attributed to PB. Timescales of different components of the recovery kinetics were determined by singular value decomposition (SVD) and attributed to various electron relaxation processes following photoexcitation. The negative TA signal of CdS thin films in the present investigation is therefore attributed mainly to PB due to the CdS absorption as well although contribution from stimulated emission (SE) cannot be completely ruled out. Unlike Ref. 12, TA spectrum of CdS in the present work does not show any positive signal in the probe region. The difference between the TA spectra of Ref. 12 and the present work may be due to different sample preparation methods and different pump wavelengths. In Ref. 12, a positive signal was observed in the short-wavelength region, namely, 10 nm (for DCPS-prepared CdS) and 20 nm (for CBD-prepared CdS) to the blue of the negative peak of the TA spectrum. The decrease of the negative signal in the short-wavelength region (<475 nm) of the CdS TA spectrum from the present experiment (Figure 4a) is therefore most probably due to the contribution from the positive PA process. At all wavelengths, the decay kinetics is almost identical with a fast and a slow time constant of ∼1 ps ∼400 ps, respectively (Figure 4b). The fast and slow decay components are attributed to donor level electron trapping and charge recombination processes, respectively.[12] Fit time constants are provided in Supplementary Information (Table S.1). TA measurement of the CdS thin films with a 775 nm pump wavelength was attempted. No TA signal was observed, ruling out the possibility of absorption to defect states.

3.4 TA spectra of CdS/CdTe thin films

TA spectra of CdS/CdTe thin films with a 775 nm pump are shown in Figure 5. The advantage of using a 775 nm pump is that, given its photon energy ($h\nu$=1.60 eV), band-to-band transition is possible only in CdTe, which simplifies the TA spectra and kinetics. The TA spectrum of as-deposited CdS/CdTe (Figure 5a) is therefore very similar to that of CdTe (Figure 3), dominated by positive PA signal of CdTe over the range of detection. However, a new feature, a dip around 480 nm (2.58 eV) is observed for the CdS/CdTe sample. By measuring the pump-energy-dependence of the depth of the dip, the possibility of nonlinear processes can be ruled out. Because of the lack of strong absorption at 775 nm by CdS (Figure 1) and the negative result from TA measurement of CdS thin films pumped at 775 nm, such a dip cannot be explained by PB or SE of CdS. It may be attributed either to PB signal due to absorption to defect states at the CdS/CdTe interface or to band filling of CdS due to electron transfer from the conduction band of CdTe to that of CdS following photoexcitation of CdTe (Figure 6), which suppresses interband transition in CdS and hence makes a negative contribution to the TA signal. The wavelength of the dip is consistent with the CdS absorption peak in the UV/visible spectrum (Figure 1) and the negative PB peak in the TA spectrum of the CdS thin film (Figure 4a), suggesting that the dominant contribution to the dip is from state filling. Note that the band gap of CdTe in the as-deposited CdS/CdTe thin film is ~1.48 eV, lower but close to the pump photon energy, and its conduction band edge is close but slightly higher than CdS (~0.31 eV),[23] which facilitates electron transfer from CdTe to CdS.

For heat-treated and $CdCl_2$-treated CdS/CdTe films, the dip at 480 nm is enhanced (Figures 5b and 5c). It is well know that post-growth annealing treatments reduce the defect states, which would decrease any possible negative PB signal due to absorption to defect states. The enhancement of the dip at 480 nm is therefore caused by more efficient electron transfer from CdTe to CdS in the treated samples.

Transient kinetics of all three samples at three probe wavelengths (480 nm, 575 nm, 700

nm) are illustrated and compared in Figure 7. Unlike the CdTe thin film (Figure 3b), decay kinetics of the positive signal of the as-deposited CdS/CdTe sample at different probe wavelengths are similar to one another. A single exponential decay with average time constant of 4.34±0.07 ps was observed. In addition, at 575 nm and 700 nm probe wavelengths, transient kinetics of all three samples are similar to one another because the positive signal in the long wavelength region is almost completely due to PA in CdTe and not affected by the treatments. The decay of the PA signal is attributed to charge trapping process, which is also observed in the TA spectra of the CdTe thin film. No slow processes like those in the CdTe thin film were observed for CdS/CdTe, suggesting the absence of recombination on this timescale.

Decay kinetics of the treated samples at 480 nm (Figure 7a) are complicated as a combination of charge carrier relaxation and charge transfer. Overall, they decay about twice as fast as the other two probe wavelengths. The transient kinetics therefore provide further evidence for enhancement of electron transfer in CdS/CdTe thin film structure upon treatments. In order to derive quantitative information of electron transfer, transient kinetics (normalized $\Delta OD(t)$) at 480 nm is subtracted from those at 700 nm. Such subtraction separates the negative contribution at 480 nm from the positive PA background. Results of the substraction ($\Delta\Delta OD$) are illustrated in Figure 8. For the as-deposited sample, the subtracted kinetics does not demonstrate decay or growth. For the treated samples, a single-exponential growth is observable, corresponding to electron transfer from CdTe to CdS, which results in the dip at 480 nm. The exponential growth is fit to a function:

$$\Delta\Delta OD(t) = \Delta\Delta OD_0 + A_0\left(1 - e^{-k_{ET}t}\right) \quad (1)$$

The electron transfer rate k_{ET} is determined to be 0.26±0.01 ps^{-1} for the heat-treated sample and 0.55±0.02 ps^{-1} for the $CdCl_2$-treated sample. The quality of the fitting (Figures 8b and 8c) confirms that the dominate contribution to the dip at 480 nm is state filling following electron transfer.

4 Conclusions

To summarize, photoinduced processes in as-deposited, heat-treated, and $CdCl_2$-treated CdS/CdTe thin films were studied by TAPPS measurements with a 775 nm (1.60 eV) pump wavelength. Aided by results from the accompanying absorption and PL measurements and using net CdTe and CdS thin films as controls, the TA spectra and kinetics were quantitatively interpreted. Band-to-band electron transition in CdTe is followed by electron transfer to CdS, which causes the 480-nm "dip" in the overall positive PA background due to CdTe absorption. Such electron transfer process has been significantly enhanced in the heat- and $CdCl_2$-treated thin films compared to the as-deposited one.

It is well known that $CdCl_2$ treatment of CdS/CdTe leads to higher efficiency in photovoltaic devices. The underlying mechanism, however, remains elusive. The present work provides a possible explanation to this phenomenon: Passivation of interface defects in treated samples enhances the CT processes and influences the competition between relaxation and CT processes. More efficient charge separation and collection is hence achieved by improved electron transfer from CdTe to CdS. Although the exact mechanism for enhancement of hole transfer is still to be explored, several facts might contribute to it. First, there is a drastic reduction of defects within CdTe upon $CdCl_2$ treatment. In a recent PL study, it was found that $CdCl_2$ treatment and annealing eliminates two out of the four defect levels and the mid-gap recombination centers are largely reduced,[24] confirming previous observations. Furthermore, UV photoemission spectroscopy[25] and X-ray photoemission spectroscopy[26] measurements showed that upon $CdCl_2$ treatment, the Fermi level of CdTe thin film is shifted close to the conduction band minimum. As a result, p-type CdTe gradually changes towards n-type and n-type CdTe (such as that used in the present work) gradually changes towards p-type. It has also been experimentally shown that this process keeps the CdTe n-type, pins the Fermi level close to the valence band maximum at the free surface of CdTe, and hence forming a large Schottky barrier.[1] The combination of the Schottky barrier and the $n-n$ heterojunction at the CdTe/CdS interface formes a strong electric field within the CdTe

layer due to the formation of a healthy depletion region in it. These two facts, in addition to re-crystallization, and reduction of grain boundaries and defects in the $CdCl_2$-treated CdS/CdTe thin film[15,19] may be used to explain the enhancement of electron transfer in such structures.

Acknowledgement

The authors gratefully acknowledge the financial support of the Department of Energy *via* its EPSCoR grant (DE-FG02-07ER46375). BP and JL acknowledge financial support from the University of Louisville. We thank Dr. Mahendra K. Sunkara for his help in the experiment and fruitful discussion.

References

(1) Dharmadasa, I.; Samantilleke, A.; Chaure, N.; Young, J. New ways of developing glass/conducting glass/CdS/CdTe/metal thin-film solar cells based on a new model. *Semicond. Sci. Tech.* **2002**, *17*, 1238–1248.

(2) Kumar, S. G.; Rao, K. S. R. K. Physics and chemistry of CdTe/CdS thin film heterojunction photovoltaic devices: fundamental and critical aspects. *Energy Environ. Sci.* **2014**, *7*, 45–102.

(3) Britt, J.; Ferekides, C. Thin-film CdS/CdTe solar cell with 15.8% efficiency. *Appl. Phys. Lett.* **1993**, *62*, 2851–2852.

(4) Wu, X. High-efficiency polycrystalline CdTe thin-film solar cells. *Sol. Energy* **2004**, *77*, 803 – 814.

(5) First Solar pushes verified CdTe cell efficiency to record 21.5%. `http://www.pv-tech.org/news/first_solar_pushes_verified_cdte_cell_efficiency_to_record_21.5`, 2015.

(6) Shah, A.; Torres, P.; Tscharner, R.; Wyrsch, N.; Keppner, H. Photovoltaic technology: the case for thin-film solar cells. *Science* **1999**, *285*, 692–698.

(7) Dobson, K. D.; Visoly-Fisher, I.; Hodes, G.; Cahen, D. Stability of CdTe/CdS thin-film solar cells. *Sol. Energy Mater. Sol. Cells* **2000**, *62*, 295 – 325.

(8) Rawalekar, S.; Kaniyankandy, S.; Verma, S.; Ghosh, H. N. Ultrafast charge carrier relaxation and charge transfer dynamics of CdTe/CdS core-shell quantum dots as studied by femtosecond transient absorption spectroscopy. *J. Phys. Chem. C* **2010**, *114*, 1460–1466.

(9) Yan, Y.; Chen, G.; Van Patten, P. G. Ultrafast exciton dynamics in CdTe nanocrystals and core/shell CdTe/CdS nanocrystals. *J. Phys. Chem. C* **2011**, *115*, 22717–22728.

(10) Wang, L.; Wang, H.-Y.; Gao, B.-R.; Pan, L.-Y.; Jiang, Y.; Chen, Q.-D.; Han, W.; Sun, H.-B. Transient absorption spectroscopic study on band-structure-type change in CdTe/CdS core-shell quantum dots. *IEEE J. Quantum. Elect.* **2011**, *47*, 1177–1184.

(11) Dooley, C. J.; Dimitrov, S. D.; Fiebig, T. Ultrafast electron transfer dynamics in CdSe/CdTe donor-acceptor nanorods. *J. Phys. Chem. C* **2008**, *112*, 12074–12076.

(12) Cooper, J. K.; Cao, J.; Zhang, J. Z. Exciton Dynamics of CdS Thin Films Produced by Chemical Bath Deposition and DC Pulse Sputtering. *ACS Appl. Mater. & Interfaces* **2013**, *5*, 7544–7551.

(13) Diso, D. G.; Muftah, G. E. A.; Patel, V.; Dharmadasa, I. M. Growth of CdS layers to develop all-electrodeposited CdS/CdTe thin-film solar cells. *J. Electrochem. Soc.* **2010**, *157*, H647–H651.

(14) Dharmadasa, R.; Dharmadasa, I.; Druffel, T. Intense Pulsed Light Sintering of Electrodeposited CdS Thin Films. *Adv. Eng. Mater.* **2014**, *16*, 1351–1361.

(15) Dharmadasa, R.; Echendu, O. K.; Dharmadasa, I.; Druffel, T. Rapid thermal processing in CdS/CdTe thin film solar cells by intense pulsed light sintering. *ECS Transactions* **2013**, *58*, 67–75.

(16) Dharmadasa, I.; Bingham, P.; Echendu, O.; Salim, H.; Druffel, T.; Dharmadasa, R.; Sumanasekera, G.; Dharmasena, R.; Dergacheva, M.; Mit, K.; Urazov, K.; Bowen, L.; Walls, M.; Abbas, A. Fabrication of CdS/CdTe-based thin film solar cells using an electrochemical technique. *Coatings* **2014**, *4*, 380–415.

(17) Hädrich, M.; Lorenz, N.; Metzner, H.; Reislöhner, U.; Mack, S.; Gossla, M.; Witthuhn, W. CdTe - CdS solar cells - Production in a new baseline and investigation of material properties. *Thin Solid Films* **2007**, *515*, 5804 – 5807.

(18) Perelaer, J.; Schubert, U. S. Novel approaches for low temperature sintering of inkjet-printed inorganic nanoparticles for roll-to-roll (R2R) applications. *J. Mater. Res.* **2013**, *28*, 564–573.

(19) Dharmadasa, R.; Lavery, B.; Dharmadasa, I. M.; Druffel, T. Intense pulsed light treatment of cadmium telluride nanoparticle-based thin films. *ACS Appl. Mater. Interfaces* **2014**, *6*, 5034–5040.

(20) Pandit, B.; Luitel, T.; Cummins, D. R.; Thapa, A. K.; Druffel, T.; Zamborini, F.; Liu, J. Spectroscopic investigation of photoinduced charge-transfer processes in FTO/TiO_2/N719 photoanodes with and without covalent attachment through silane-based linkers. *J. Phys. Chem. A* **2013**, *117*, 13513–13523.

(21) Sze, S. *Physics of Semiconductor Device*; Wiley Interscience: New York, 1981.

(22) Jenny, D. A.; Bube, R. H. Semiconducting Cadmium Telluride. *Phys. Rev.* **1954**, *96*, 1190–1191.

(23) Gao, J.-N.; Jie, W.-Q.; Yuan, Y.-Y.; Zha, G.-Q.; Xu, L.-Y.; Wu, H.; Wang, Y.-B.; Yu, H.; Zhu, J.-F. In-situ SRPES study on the band alignment of (0001)CdS/CdTe heterojunction. *Chin. Phys. Lett.* **2012**, *29*, 057301.

(24) Dharmadasa, I. M.; Echendu, O. K.; Fauzi, F.; Abdul-Manaf, N. A.; Salim, H. I.; Druffel, T.; Dharmadasa, R.; Lavery, B. Effects of $CdCl_2$ treatment on deep levels in CdTe and their implications on thin film solar cells; A comprehensive photoluminescence study. *J. Mater. Sci. - Mater. El.* **in press**,

(25) Dharmadasa, I. M.; Echendu, O. K.; Fauzi, F.; Salim, H. I.; Abdul-Manaf, N. A.; Jasinski, J. B.; Sherehiy, A.; Sumanasekera, G. Study of Fermi level movement during $CdCl_2$ treatment of CdTe thin films using Ultra-violet Photoemission Spectroscopy. **submitted**,

(26) Schulmeyer, T.; Fritsche, J.; Thißen, A.; Klein, A.; Jaegermann, W.; Campo, M.; Beier, J. Effect of in situ UHV $CdCl_2$-activation on the electronic properties of CdTe thin film solar cells. *Thin Solid Films* **2003**, *431-432*, 84 – 89.

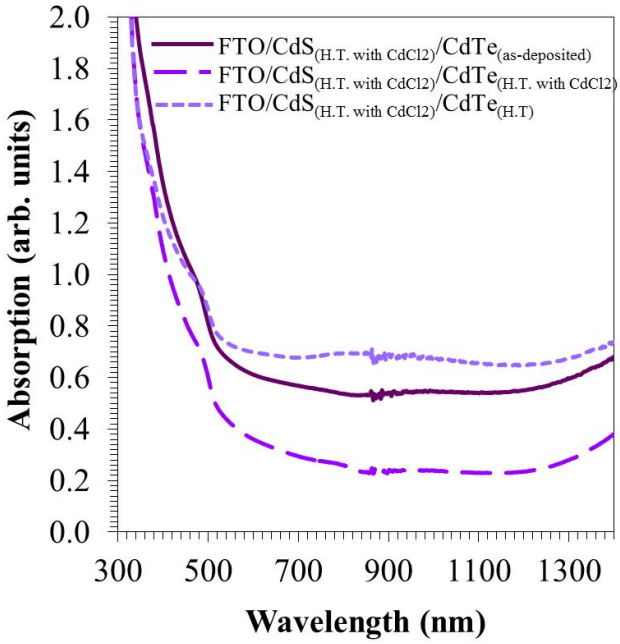

Figure 1: UV/visible/near-IR absorption spectra of CdS/CdTe thin films.

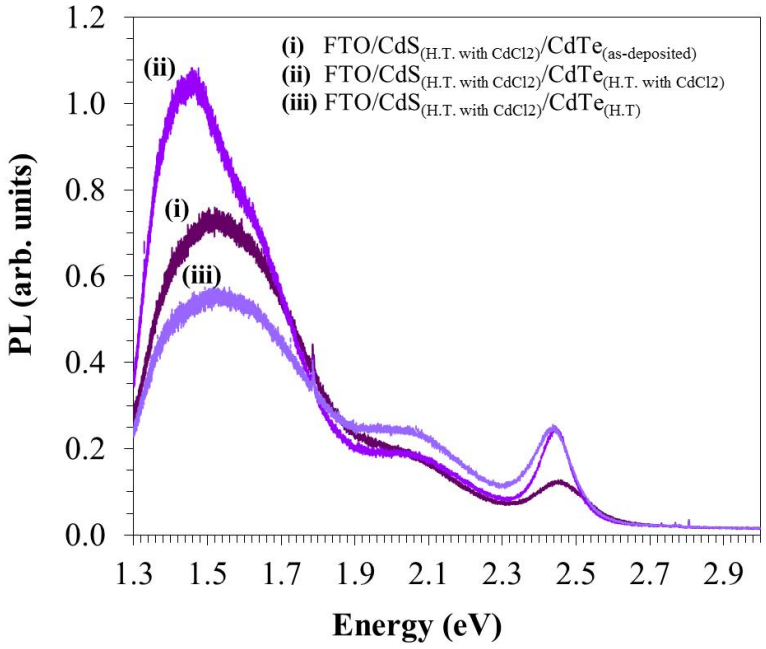

Figure 2: Photoluminescence (PL) spectra of CdS/CdTe thin films with a 442 nm (2.81 eV) excitation.

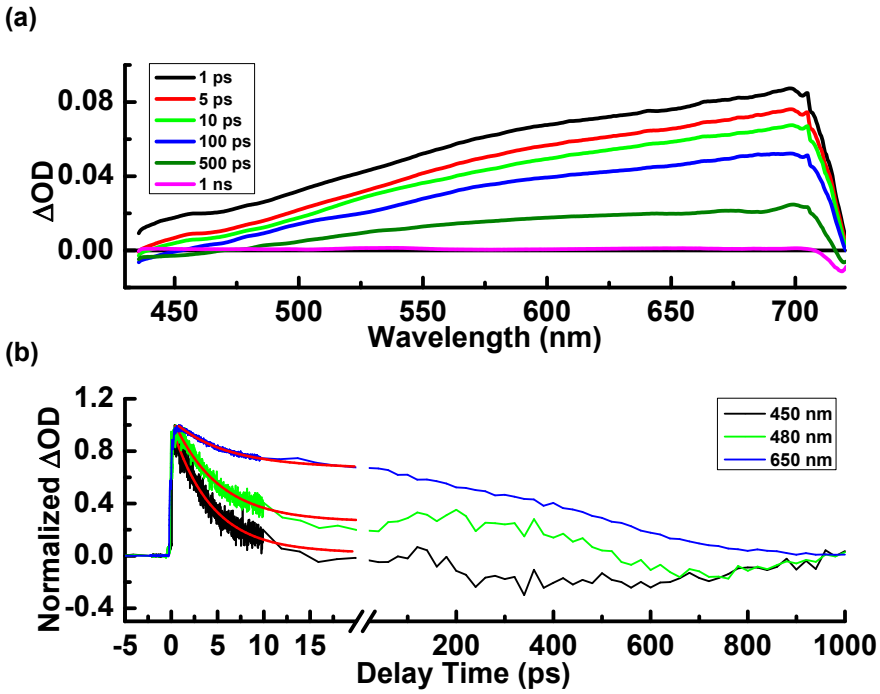

Figure 3: (a) TA spectra of CdTe thin films at Δt=1, 5, 10, 100, 500, and 1000 ps with a 775 nm pump wavelength. (b) Normalized transient kinetics at 450 nm, 480 nm, and 650 nm probe wavelengths. Red lines represent the simulation of exponential decay in the first delay time region of 0-20 ps. The fit time constants are 4.25±0.11 ps, 4.93±0.11 ps, and 5.55±0.10 ps for 450 nm, 480 nm, and 650 nm decay kinetics, respectively.

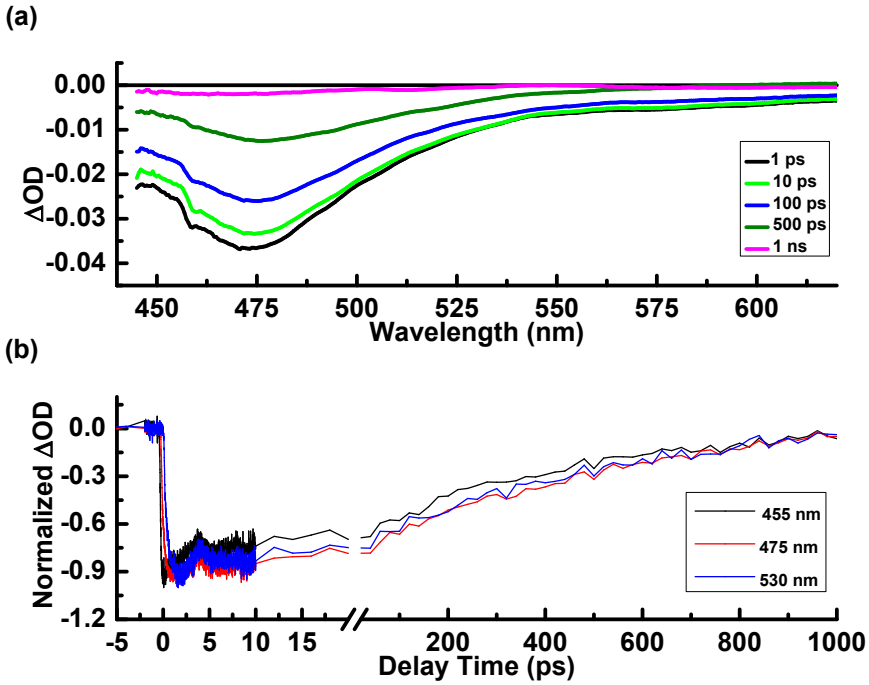

Figure 4: (a) TA spectra of CdS thin films at Δt=1, 10, 100, 500, and 1000 ps with a 388 nm pump wavelength. (b) Normalized transient kinetics at 455 nm, 475 nm and 530 nm probe wavelengths.

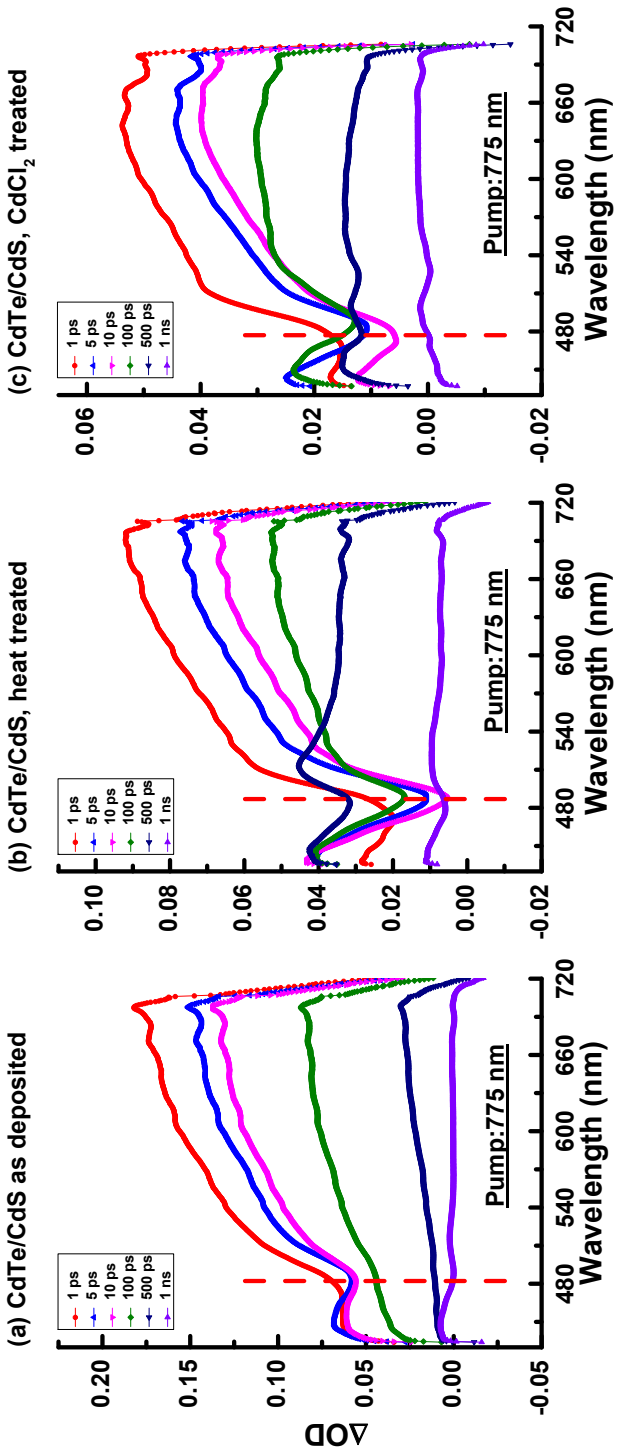

Figure 5: TA spectra of (a) as-deposited, (b) heat-treated, and (c) $CdCl_2$-treated CdS/CdTe thin films with a 775 nm pump wavelength.

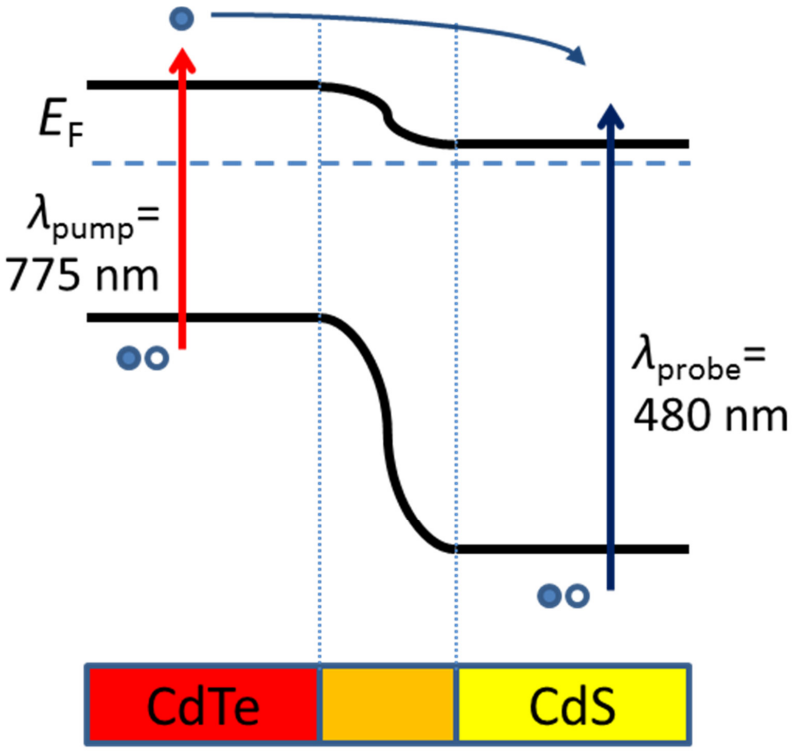

Figure 6: Schematic diagram of band structure, photoexcitation, and charge transfer process in CdS/CdTe thin films.

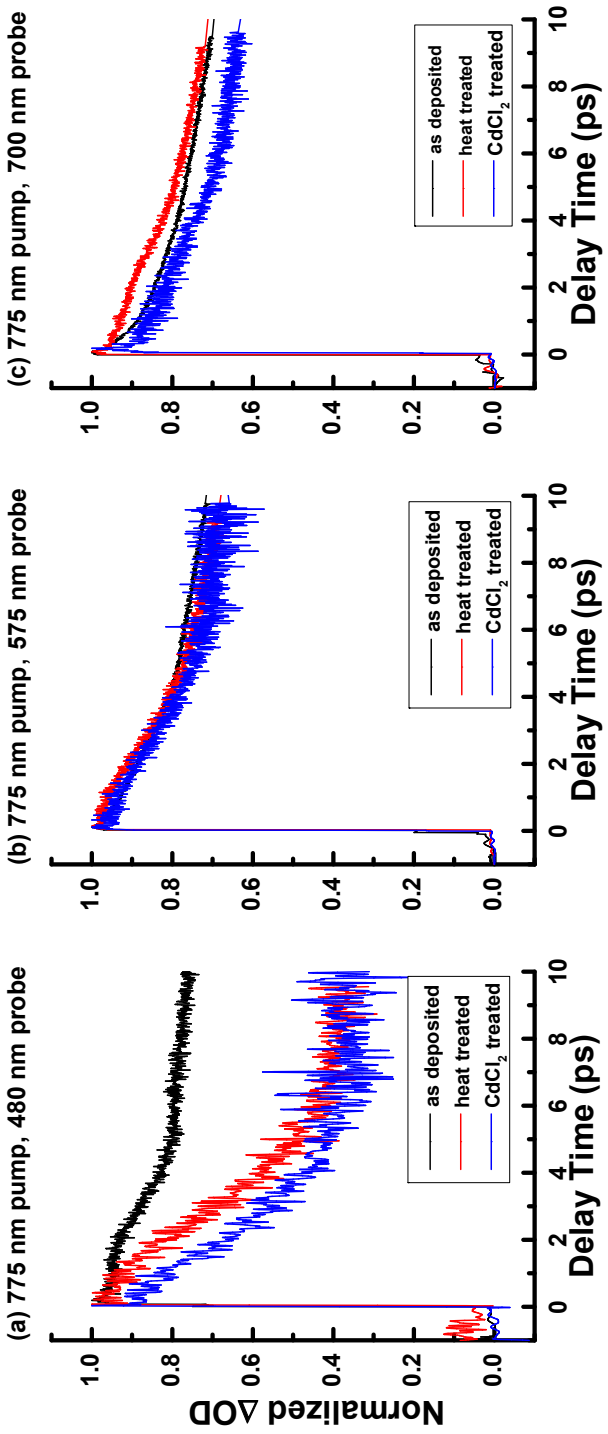

Figure 7: Normalized transient kinetics of CdS/CdTe thin films at (a) 480 nm, (b) 575 nm, and (c) 700 nm probe wavelengths with a 775 nm pump wavelength.

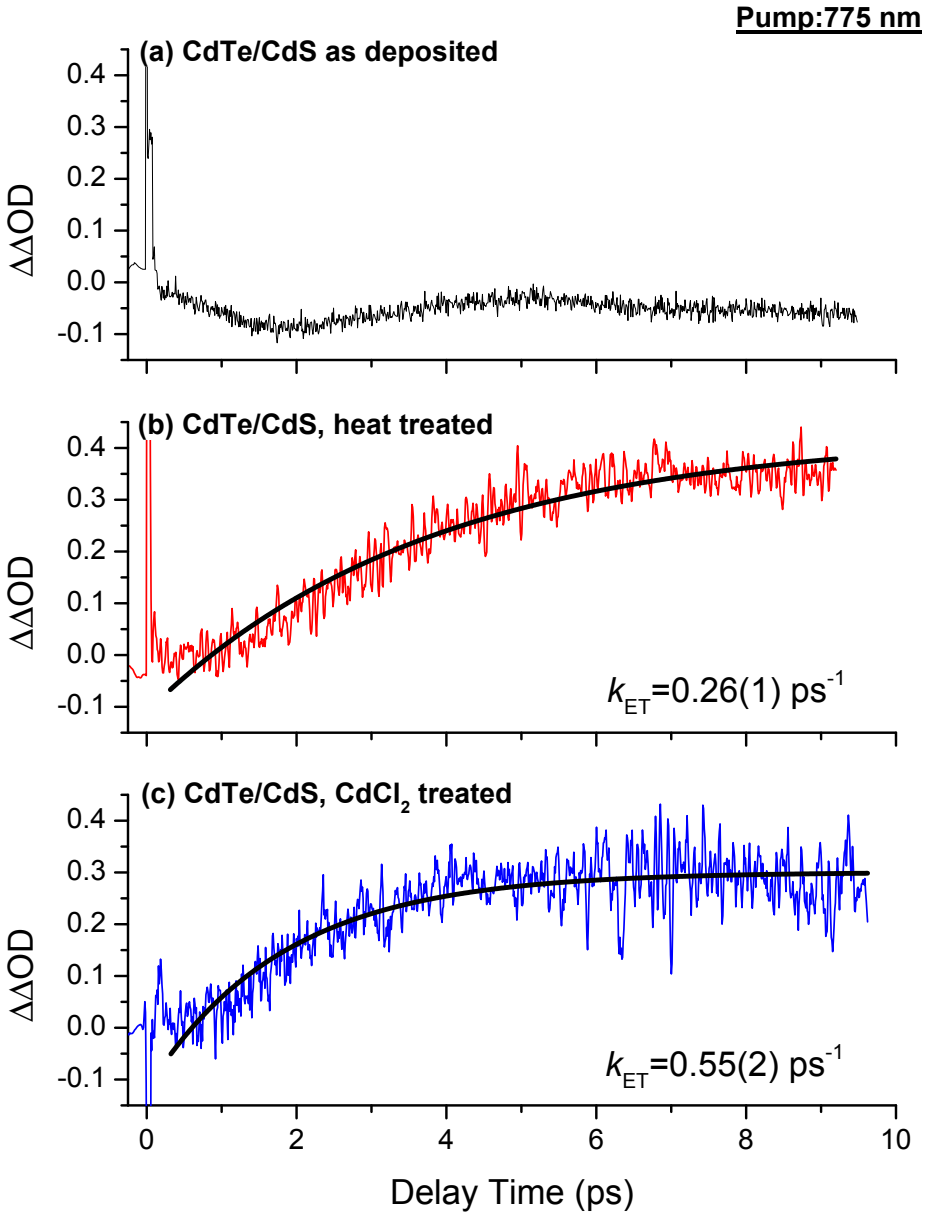

Figure 8: Subtraction of kinetics at 480 nm (Figure 7a) from that at 700 nm (Figure 7c) of (a) as-deposited; (b) heat-treated, and (c) $CdCl_2$-treated CdS/CdTe thin films with a 775 nm pump wavelength. $\Delta\Delta OD = \Delta OD_{700nm} - \Delta OD_{480nm}$. The thick dark lines are fit kinetics that represents the electron transfer as described in the text.